Geomechanics and Engineering, *Vol. 25, No. 2 (2021) 75-87*
DOI: https://doi.org/10.12989/gae.2021.25.2.075

Modelling the hydraulic/mechanical behaviour of an unsaturated completely decomposed granite under various conditions

Xi Xiong[1], Yonglin Xiong*[2] and Feng Zhang[3]

[1]*Institute of Science and Engineering, Faculty of Geoscience and Civil Engineering, Kanazawa University, Kanazawa, Ishikawa 920-1192, Japan*
[2]*Institute of Geotechnical Engineering, Ningbo University, Ningbo 315211, China*
[3]*Department of Civil Engineering, Nagoya Institute of Technology, Showa-ku, Gokiso-cho, Nagoya 466-8555, Japan*

(Received January 29, 2021, Revised March 16, 2021, Accepted March 21, 2021)

Abstract. Because the hydraulic/mechanical behaviour of unsaturated soil is more complicated than that of saturated soil, one of the most important issues in modelling unsaturated soil is to properly couple its stress-strain relationship with its water retention characteristics. Based on the results of a series of tests, the stress-strain relationship and the changes in suction and saturation of unsaturated completely decomposed granite (CDG, also called Masado) vary substantially under different loading/hydraulic conditions. To precisely model the hydraulic/mechanical behaviour of unsaturated Masado, in this study, the superloading concept was firstly introduced into an existing saturated/unsaturated constitutive model to consider the structural influences. Then a water retention curve (WRC) model considering the volumetric change in the soil, in which the skeleton and scanning curves of the water retention characteristics were assumed to shift in parallel in accordance with the change in the void ratio, was proposed. The proposed WRC model was incorporated into the constitutive model, and the validity of the newly proposed model was verified using the results of tests conducted on unsaturated Masado, including water retention, oedometer and triaxial tests. The accuracy of the proposed model in describing the stress-strain relationship and the variations in suction and saturation of unsaturated Masado is satisfactory.

Keywords: unsaturated soil; completely decomposed granite; constitutive model; water retention curve model; water retention test; oedometer test; triaxial test

1. Introduction

Completely decomposed granite (CDG), which is usually called Masado in Japanese geotechnical engineering, is a typical sandy soil that can be found widely in western Japan. Because Masado is well graded and can be easily compacted, it is often used as a reclaimed material for road construction. However, changes in the water content or the degree of saturation S_r can lead to very large variations in the strength and deformation of unsaturated Masado (Xiong 2020). As a result, one of the major causes of the failure of slopes that are made of either natural Masado (cut slope) or manmade Masado (reclaimed slope) is heavy rainfall (Murata *et al.* 1988, Li and Cameron 2002, Sehara *et al.* 2006, Kawamura and Miura 2018). Based on the results of a series of tests on unsaturated Masado, the stress-strain relationship and the changes in suction and saturation of Masado vary substantially under different loading/hydraulic conditions (Xiong, 2020). Therefore, to precisely model the hydraulic/mechanical behaviour of unsaturated Masado, it is of great importance to propose a saturated/unsaturated soil constitutive model coupled with a proper water retention curve (WRC).

A completely hydraulic/mechanical coupled constitutive model for unsaturated soil was first proposed by Vaunat *et al.* (2000). Thereafter, many efforts had been made to propose a saturated/unsaturated soil constitutive model with a WRC to properly consider the degree of saturation S_r (or volumetric water content, w) and suction s, e.g., the works by Sheng *et al*. (2004), Zhang and Ikariya (2011). It has been observed in many experiments, however, that the deformation of soil may influence the water retention behaviour (e.g., Miller *et al.* 2008, Romero *et al.* 2011, Salager *et al.* 2013, Seiphoori *et al.* 2014 and Sun *et al.* 2014, Gao *et al.* 2018, Gao *et al.* 2021). Recent studies show that not only the degree of saturation but also the suction is influenced by the deformation of unsaturated soil (Burton *et al.* 2016, Xiong *et al.* 2019 and Xiong 2020). From these studies, it is concluded that the separate treatment of the mechanical and hydraulic components in modelling unsaturated soil behaviour has limitations in reproducing the experimental observations (Sheng 2011). Therefore, it is necessary to properly consider the influence of soil deformation when modelling water retention behaviour characteristics.

In recent studies, the influence of the deformation of unsaturated soils on the water retention behaviour is usually modelled via a deformation-dependent WRC. Certain WRC models are in good agreement with most of the main tested drying or wetting curves at different void ratios, while hysteresis in water retention behaviour is ignored (e.g.,

*Corresponding author, Associate Professor
E-mail: xiongyonglin@nbu.edu.cn

ISSN: 2005-307X (Print), 2092-6219 (Online)

Gallipoli *et al.* 2003, Khoshghalb *et al.* 2015, Tan *et al.* 2016, Wijaya and Leong 2017). Generally, the existing hysteretic WRCc models were proposed by relating the air entry value and/or variation in the degree of saturation to the soil density (Sun *et al.* 2007, Zhou and Sheng 2015), soil volume (Tarantino 2009, Sheng and Zhou 2011), volumetric strain (Nuth and Laloui 2008), and pore-size distribution (Maqsoud *et al.* 2012, Hu *et al.* 2013). According to a previous experimental study (Henkel, 1960), however, the change in void ratio is independent of the stress path, which has been used as a state variable in many constitutive models (e.g., Zhang and Ikariya 2011, Xiong *et al.* 2019). Therefore, to establish a deformation-dependent WRC model, it is also reasonable to relate the variation in saturation to the change in void ratio. Gallipoli (2012) and Gallipoli *et al.* (2015) presented a hysteretic WRC model by incorporating a power function of the void ratio in the van Genuchten model (van Genuchten, 1980). In the work of Pasha *et al.* (2017), a model for evaluating the void ratio dependency of the WRC in deformable porous media was proposed.

In the aforementioned studies, however, most deformation-dependent WRC models were only validated against the tested hydraulic behaviour (S_r-s relation) of unsaturated soil. Only a few of the models were coupled with constitutive models and evaluated by comparing the simulated and tested hydraulic/mechanical behaviour (S_r-stress-strain and s-stress-strain relations). In addition, the number of studies on the influence of structure on deformation and the influence of the strength of unsaturated soils, which has been observed in Masado (Tsuchida *et al.* 2011), is limited. Therefore, in this study, the superloading concept was first introduced into an existing saturated/unsaturated constitutive model (Zhang and Ikariya, 2011) using the degree of saturation and the Bishop-type skeleton stress as state variables to consider the influences of the structure. Then a WRC model was proposed to account for the influences of deformation and hysteresis on the variations in saturation and suction. Finally, the proposed WRC model was incorporated into the constitutive model, and the validity of the newly proposed model was carefully verified using the results of tests conducted on unsaturated Masado, including water retention, oedometer and triaxial tests (Xiong 2020).

2. Derivation of constitutive model

2.1 Yield function

To model the hydraulic/mechanical behaviour of unsaturated Masado, a constitutive model (Zhang and Ikariya 2011) for saturated/unsaturated soil was selected. Based on experimental results, Zhang and Ikariya (2011) proposed a saturated/unsaturated constitutive model using the skeleton stress and the degree of saturation as independent variables. The skeleton stress, a type of Bishop-type effective stress, is defined as follows:

$$\sigma''_{ij} = \sigma^t_{ij} - u_a\delta_{ij} + S_r(u_a - u_w)\delta_{ij} = \sigma^n_{ij} + S_r s\delta_{ij} \quad (1)$$

For simplicity, throughout the context, the skeleton stress tensor σ''_{ij} is abbreviated as σ_{ij} without

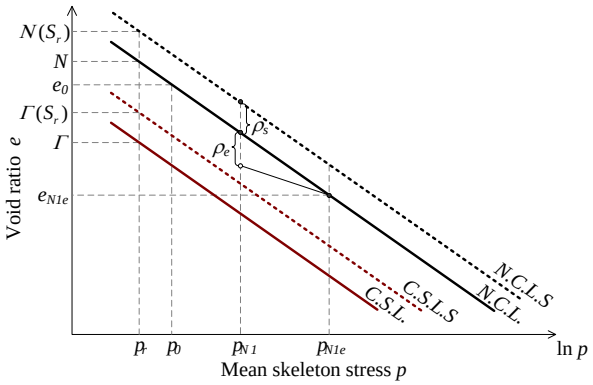

Fig. 1 e–ln p relationship based on raising the *N.C.L.* and the critical state line (*C.S.L.*) due to instauration (Zhang and Ikariya 2011)

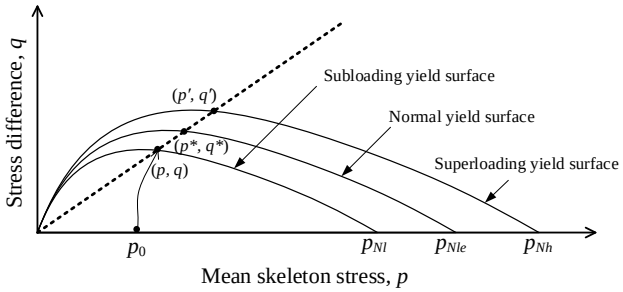

Fig. 2 Subloading, normal and superloading yield surfaces in the p-q plane

specification in the following context.

In this constitutive model, it is assumed that the normally consolidated line in the unsaturated state (*N.C.L.S.*) is parallel to the normally consolidated line in the saturated state (*N.C.L.*) but at a higher position than the *N.C.L.*, as shown in Fig. 1. $N(S_r)$ and $\Gamma(S_r)$ are the void ratios at *N.C.L.S.* and the critical state line in the unsaturated state (*C.S.L.S.*), respectively, under a reference mean skeleton stress p_r. Furthermore, the overconsolidation of soil is also properly described based on the concept of subloading (Hashiguchi and Ueno 1977).

In this study, to accurately describe the deformation and strength of unsaturated soil, the concept of superloading (Asaoka *et al.* 1998, Asaoka *et al.* 2000) was added into the present constitutive model (Zhang and Ikariya 2011) to properly consider the soil structure. The subloading, normal and superloading yield surfaces are shown in Fig. 2, and their intersections with the p-axis are p_{Nl}, p_{Nle} and p_{Nh}, respectively. The similarity ratio of the superloading yield surface to the normal yield surface R^* and the similarity ratio of the superloading yield surface to the subloading yield surface R are defined as follows:

$$R^* = \frac{p^*}{p'} = \frac{q^*}{q'},\ 0 < R^* \le 1 \text{ and } \frac{q^*}{p^*} = \frac{q'}{p'} \quad (2)$$

$$R = \frac{p}{p'} = \frac{q}{q'},\ 0 < R \le 1,\ R = \frac{1}{OCR} \text{ and } \frac{q}{p} = \frac{q^*}{p^*} = \frac{q'}{p'} \quad (3)$$

where, (p, q), (p^*, q^*) and (p', q') represent the present stress state, the corresponding normally consolidated stress state and the structured stress state at p-q plane, respectively.

The yield function can be obtained as

$$f=\ln\frac{p}{p_0}+\ln\frac{M^2+\eta^2}{M^2}+\frac{\rho_e}{1+e_0}\frac{1}{C_p}-\frac{\rho^*}{1+e_0}\frac{1}{C_p}-\frac{\rho_s}{1+e_0}\frac{1}{C_p}-\varepsilon_v^p\frac{1}{C_p}=0 \tag{4}$$

where

$$C_p=\frac{\lambda\text{-}\kappa}{1+e_0},\quad \rho^*=(\lambda-\kappa)\ln\frac{1}{R^*},\quad \rho_s=N(S_r)-N,\quad \rho_e=(\lambda-\kappa)\ln\frac{1}{R} \tag{5}$$

p_0 is the reference mean skeleton stress, ε_v^p is the plastic volumetric strain, η is the stress ratio and M is the stress ratio at the critical state. λ is the compression index, and κ is the swelling index. ρ_* represents a void ratio difference between the normally consolidated state and the structured state under the same mean skeleton stress. ρ_s represents a void ratio difference between *N.C.L.* and *N.C.L.S.* under the same mean skeleton stress. $N(S_r)$ and N are the void ratio at a value of S_r and at full saturation under the reference mean skeleton stress, respectively. ρ_e represents a void ratio difference between the normally consolidated state and the overconsolidated state under the same mean skeleton stress.

An associated flow rule is employed in the model, namely,

$$d\varepsilon_{ij}^p=\Lambda\frac{\partial f}{\partial\sigma_{ij}} \tag{6}$$

where Λ is the plastic scalar factor.

From the consistency equation df=0, the consistency equation for the yield surface can then be given as:

$$df=\frac{\partial f_\sigma}{\partial\sigma_{ij}}d\sigma_{ij}+d(\frac{\rho_e}{1+e_0})\frac{1}{C_p}-d(\frac{\rho^*}{1+e_0})\frac{1}{C_p}-d(\frac{\rho_s}{1+e_0})\frac{1}{C_p}-d\varepsilon_v^p\frac{1}{C_p}=0 \tag{7}$$

It is clear that the evolution rule for the development of the state variables ρ_e of overconsolidation, ρ^* of structure and ρ_s of saturation should be given in advance in order to obtain the plastic deformation.

2.2 Evolution rules

The evolution equations for the development of the state variables ρ^* of structure, ρ_e of overconsolidation and ρ_s of saturation are given as follows:

$$d(\frac{\rho_e}{1+e_0})=-\Lambda\frac{\rho^\beta}{\sigma_{mm}},\quad \rho=a\rho_e+b\rho_s \tag{8}$$

$$d(\frac{\rho^*}{1+e_0})=e^{b\rho_s}(1-e^{m^*\rho^*})Md\varepsilon_d^p \tag{9}$$

$$\begin{cases}N(S_r)=N+\dfrac{N_r-N}{S_r^s-S_r^r}(S_r^s-S_r);N_r=N(S_r^r)\\ \rho_s=N(S_r)-N=Q(S_r^s-S_r);Q=\dfrac{N_r-N}{S_r^s-S_r^r}\\ d\rho_s=-QdS_r\end{cases} \tag{10}$$

where e is Napier's constant, ε_d^p is the plastic shear strain, m^* is a parameter that controls the rate of collapse of the structure during shearing, S^r_r and S^s_r are the degree of saturation under residual and saturated conditions, respectively, parameters a, b and β control the development of the state variables ρ_e and ρ^* and N_r is the void ratios at *N.C.L.S.* under the reference mean skeleton stress p_r when the degree of saturation is in the residual state, that is, N_r=$N(S^r_r)$, as shown in Fig. 1.

ε^p_d is denoted as

$$d\varepsilon_d^p=\Lambda\frac{\partial f}{\partial q}=\Lambda\frac{1}{M}\frac{1}{\sigma_{mm}} \tag{11}$$

Substituting Eq. (11) into Eq. (9), the evolution equation for the development of ρ^* can be determined as

$$d(\frac{\rho^*}{1+e_0})=e^{b\rho_s}(1-e^{m^*\rho^*})\Lambda\frac{1}{\sigma_{mm}} \tag{12}$$

2.3 Plastic scalar factor and loading criteria

Substituting Eqs. (8), (10) and (12) into Eq. (7), the valuable Λ can be determined as:

$$\Lambda=\frac{\dfrac{\partial f}{\partial\sigma_{ij}}d\sigma_{ij}+\dfrac{1}{C_p}\dfrac{Q}{1+e_0}dS_r}{\dfrac{1}{C_p}\dfrac{\rho^\beta}{\sigma_{mm}}+\dfrac{1}{C_p}e^{b\rho_s}(1-e^{m^*\rho^*})\dfrac{1}{\sigma_{mm}}+\dfrac{1}{C_p}\dfrac{\partial f}{\partial\sigma_{mm}}}=\frac{\dfrac{\partial f}{\partial\sigma_{ij}}E_{ijkl}d\varepsilon_{kl}+\dfrac{1}{C_p}\dfrac{Q}{1+e_0}dS_r}{\dfrac{h_p}{C_p}} \tag{13}$$

where

$$h_p=\frac{\rho^\beta+e^{b\rho_s}(1-e^{m^*\rho^*})}{\sigma_{mm}}+\frac{\partial f}{\partial\sigma_{mm}} \tag{14}$$

The loading criteria are given according to Zhang and Ikariya (2011), as shown below:

$$\begin{cases}\Lambda>0 & \text{Loading}\\ \Lambda=0 & \text{Neutral loading}\\ \Lambda<0 & \text{Unloading}\end{cases} \tag{15}$$

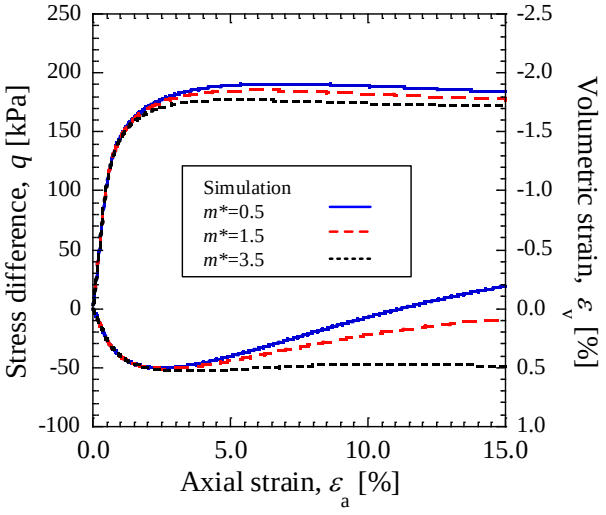

Fig. 3 Influence of structure parameter m^* on the skeleton stress, strain and dilatancy relations

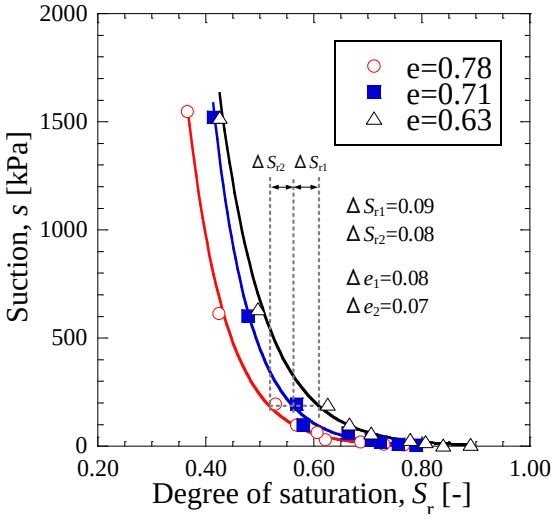

Fig. 4 WRC of loam at constant void ratios (data from Sugii *et al.* 2002)

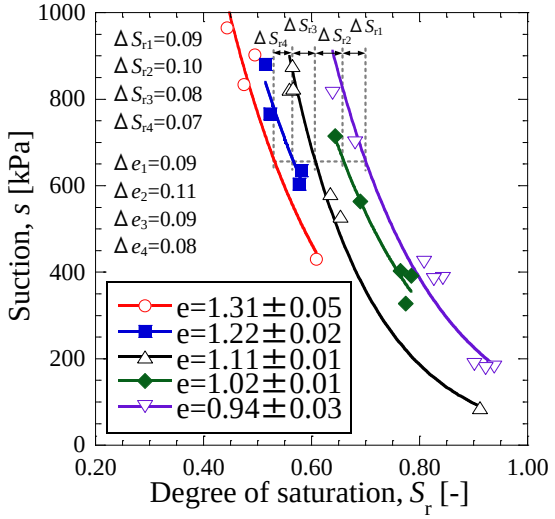

Fig. 5 WRC of compacted Speswhite kaolin at nearly constant void ratios (data from Tarantino 2009)

2.4 Model parameters

The constitutive model includes ten material parameters, five of which, M, N, λ, κ and ν, have the same meanings as those of the Cam-Clay model. Parameters a, b and β control the degree of over consolidation and can be determined by triaxial tests. N_r is the void ratio at *N.C.L.S.* under reference mean skeleton stress p_r when the degree of saturation is in the residual state. The newly added parameter m^* controls the rate of collapse of the structure during shearing and can also be determined by triaxial tests.

Fig. 3 shows the simulated skeleton stress, strain and dilatancy relations in triaxial compression tests on unsaturated soil under drained-vented conditions with the same initial structure state value ρ^*=0.3. During shearing, the confining stress and the suction were kept constant. Based on the figure, as m^* increases, both the peak strength and the dilatancy of the soil decrease, which means the rate of collapse of the structure increases.

3. Water retention curve model considering volumetric change

3.1 Experimental evidence

The WRC, also called the soil water characteristic curve (SWCC), is different for different types of soils. There are several methods to obtain the WRC for different suction ranges, e.g., the axis-translation, osmotic and vapour equilibrium methods. Measuring the volumetric change in unsaturated specimens induced by suction loading in the WRC test is essential to investigate the deformation dependency of the WRC.

Xiong (2020) conducted water retention tests on Masado using a custom designed oedometer test apparatus with the axis-translation method. Both the suction and vertical displacement were measured during the entire loading/unloading process. The test results show that the WRC of Masado moves towards a higher degree of saturation with decreasing void ratio, which is similar to the phenomenon observed by Salager *et al.* (2013). The obtained WRC clearly shows the concurrent influences of suction and deformation on the degree of saturation. In modelling the deformation dependency of the WRC, however, it is essential to quantify their effects individually.

Nuth and Laloui (2008) first proposed an intrinsic WRC that describes the water retention capacity of soil with a constant porosity. Although controlling the porosity in WRC tests is difficult, the WRCs with different initial states were rearranged according to a fixed void ratio in certain studies, e.g., Sugii *et al.* (2002) and Tarantino (2009). Interestingly, an intrinsic shape is common for each of the void ratios within the ranges of concern, as shown in Figs. 4 and 5. In addition, by comparing the shifting values ΔS_r of the intrinsic WRC along the S_r axis and the variations in void ratio Δe, it is found that the shifting values ΔS_r increase with increasing void ratio Δe.

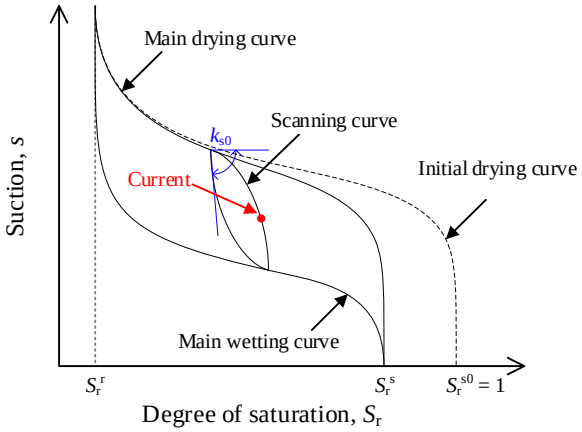

Fig. 6 WRC model considering hysteresis (Zhang and Ikariya 2011)

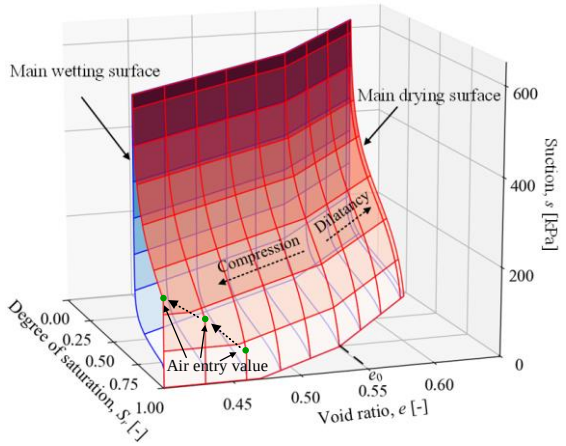

Fig. 7 Newly proposed main drying/wetting surfaces in S_r-e-s space

Based on the experimental evidence described above, in this study, the following two assumptions were made:

(a) An intrinsic WRC at any void ratio could be determined by a simple parallel shift of the intrinsic WRC at a reference void ratio along the S_r axis in S_r-s space, and

(b) The shifting value ΔS_r of the intrinsic WRC along the S_r axis follows a linear relationship with the variation in void ratio Δe.

3.2 Skeleton and scanning curves

In the unsaturated soil constitutive model (Zhang and Ikariya, 2011), a WRC model using arctangent functions as its skeleton curves, as shown in Fig. 6, was adopted. Thus, in any moisture state (S_r, s), it is possible to obtain the incremental relationship between suction and degree of saturation as:

$$dS_r = k_s^{-1} ds \tag{16}$$

where k_s is the tangential stiffness of the suction-saturation curve. Eq. (16) was used to describe the intrinsic WRC in this study.

As noted by Tarantino (2009), the degree of saturation may change because of water flowing in/out of the soil (hydraulic path) or a change in the void ratio (mechanical path). From this viewpoint, the incremental saturation was assumed to be composed of two parts, dS^s_r and dS^e_r, of which dS^s_r is attributed to removing water from the soil and dS^e_r is attributed to the change in void ratio de. In addition, according to the abovementioned assumptions, a new WRC model is obtained:

$$dS_r = dS_r^s + dS_r^e = k_s^{-1} ds + c_e de \tag{17}$$

where c_e is a parameter corresponding to the change in void ratio. When the void ratio remains constant, the proposed model has the same expression as Equation (16). Moreover, from a micro-perspective, water can also flow into or out of pores during soil deformation. Considering the difference in the contact angle between the water flowing into and out of pores, it is reasonable to assume that the value of c_e under compression and dilatancy conditions should be different.

By introducing c_e, the skeleton curves of the WRC model (Zhang and Ikariya, 2011) can be modified simply and naturally as follows:

(a) Main drying curve

$$S_r = S_r^s - \frac{2}{\pi}(S_r^s - S_r^r)\arctan((e^{c_1 s} - 1)/e^{c_1 S_d}) - c_e(e - e_0) \tag{18}$$

(b) Main wetting curve

$$S_r = S_r^s - \frac{2}{\pi}(S_r^s - S_r^r)\arctan((e^{c_2 s} - 1)/e^{c_2 S_w}) - c_e(e - e_0) \tag{19}$$

where e is Napier's constant. c_1 and c_2 are scaling factors that control the intrinsic shape of the curves, while S^s_r, S^r_r, S_d and S_w have definite physical meanings. S^s_r and S^r_r are the degrees of saturation under residual and saturated conditions, respectively. S_d is a parameter corresponding to the drying air entry value, and S_w is a parameter corresponding to the wetting air entry value.

Fig. 7 shows the main drying/wetting surfaces defined by Eqs. (18) and (19) in S_r-e-s space. Although the saturated and residual degrees of saturation of the WRC, S^s_r and S^r_r, respectively, increase as the void ratio decreases, the degree of saturation cannot be higher than 1.0.As a result, after S^s_r reaches 1.0, the intersection point of the main drying curve and the surface S_r =1.0 can be regarded as the air entry value, which increases as the void ratio decreases. In other words, the proposed model could also describe the influence of deformation on the air entry value, which has been observed in many experiments, e.g., Salager *et al.* (2013) and Seiphoori *et al.* (2014).

Regarding the scanning curve, the incremental relation between suction and saturation is expressed as:

$$k_s = \begin{cases} k_w + k_{d\max} r^{I_d} & ds \geq 0 \\ k_w + k_{d\max} r^{Iw} & ds < 0 \end{cases} \tag{20}$$

where k_w is the gradient of the corresponding main wetting curve under the same suction condition, k_{dmax} is the gradient of the main drying curve under the residual condition, and I_d and I_w are scaling factors controlling the curvature of the scanning curve in the drying and wetting processes,

respectively. The inner variable r is defined as:

$$r = s / s_{\max} \tag{21}$$

where s_{max} is the suction under the residual condition. Moreover, the values of k_w, k_{dmax} and s_{max} can be determined from Equations (18) and (19), and only I_d and I_w are model parameters. Substituting Equations (20) and (21) into Eq. (17), the scanning curve between the skeleton curves can be derived accounting for the effect of the change in void ratio. It should be emphasized that there are three characteristic scanning curves under specific conditions. According to Eq. (17),

(a) Constant suction (CS) condition, ds=0

$$dS_{\mathrm{r}} = c_e de \tag{21}$$

(b) Constant degree of saturation (CDS) condition, dS_{r}=0

$$ds = -k_s c_e de \tag{22}$$

(c) Undrained/unvented (u/u) condition, dw=0

$$S_{\mathrm{r}} = \frac{wG_s}{e} \Rightarrow dS_{\mathrm{r}} = \frac{G_s dw + S_{\mathrm{r}} de}{e} = \frac{S_{\mathrm{r}} de}{e} \tag{23}$$

$$ds = \left(\frac{S_{\mathrm{r}}}{e} - c_e\right) k_s de \tag{24}$$

where w is the water content and G_s is the specific gravity. By the abovementioned equations, the proposed WRC model can describe the variations in suction and saturation both under drained/vented and u/u conditions. In addition, these three characteristic scanning curves are important to determine the parameter values of the proposed WRC model.

This WRC model is based on the assumptions in Section 3.1. In other words, the WRC model is considered to be suitable for soils with suctions of less than 1500 kPa at the residual degree of saturation sate, such as Masado. For soils with a wider suction range, such as those in the test results presented by Chen *et al.* (2020), further studies are necessary.

3.3 Model parameters

Nine parameters are involved in the proposed WRC model, among which six parameters, c_1, c_2, $S^{\mathrm{s}}_{\mathrm{r}}$, $S^{\mathrm{r}}_{\mathrm{r}}$, S_d and S_w, can be determined in the same way as was done in the work by Zhang and Ikariya (2011). The newly added parameter, c_e, can be determined by the intrinsic WRC at different void ratios from water retention tests. In determining the intrinsic shape of the WRC using the water retention test, c_e is first determined by fitting the S_{r}-e-s relationships in the skeleton curves from water retention tests or triaxial compression tests under specific hydraulic/mechanical conditions, e.g., CS, CDS or u/u conditions, in which all suction, drainage discharge and deformation of a specimen are measured. After the value of c_e is determined, I_d and I_w can then be determined by fitting the obtained S_{r}-e-s relations of the scanning curves from water retention tests.

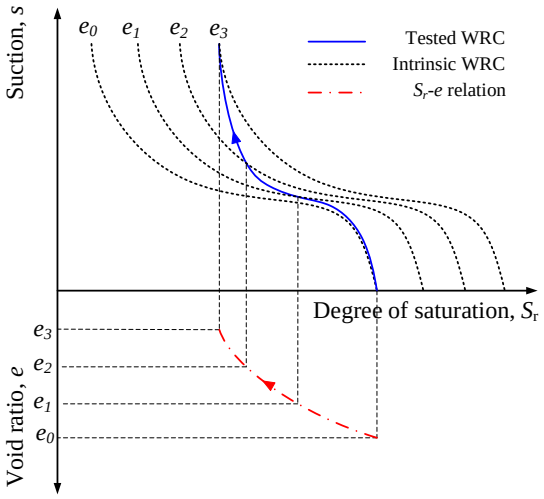

Fig. 8 Parallel shift of the WRC in S_{r}-s space due to compression and the compound relations with ds and de

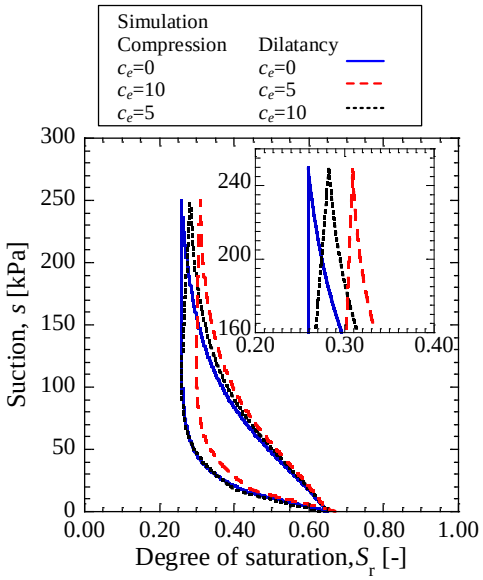

Fig. 9 Influence of parameter c_e on the skeleton curve of the WRC

Fig. 8 depicts the drying process in a water retention test with a deformable soil whose compound relation with ds and de is illustrated based on the assumption of a parallel shift of the intrinsic WRC due to the change in void ratio de in S_{r}-s space. It is concluded from the figure that the shape of the real WRC diverges from the reference intrinsic shape, and point (S_{r}, s) continually jumps from one intrinsic curve to another. As a result, the compound relation in S_{r}-s space is expressed by the blue solid line. In other words, by coupling the proposed WRC with the abovementioned constitutive model, it is possible to describe the S_{r}-e-s relation properly.

To investigate the influence of the newly added parameters on the WRC, c_e, I_d and I_w were assigned various values, and the water retention tests were simulated using the proposed model together with the proposed constitutive model. Fig. 9 shows the influence of parameter c_e on the

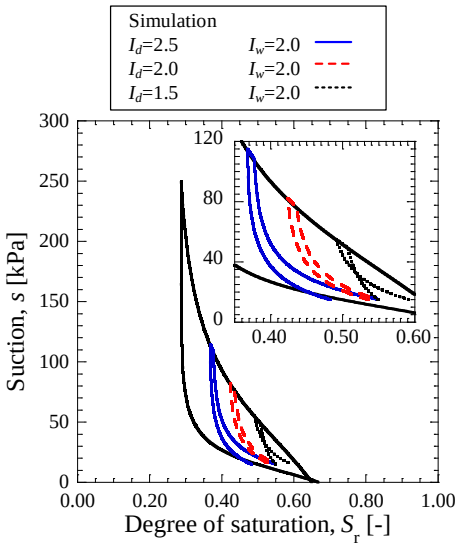

Fig. 10 Influence of parameters I_d and I_w on the scanning curve of the WRC

skeleton curve of the WRC for deformable soil. In these element simulations, the initial condition is the same, that is, the initial suction s_0=0 kPa, the initial degree of saturation S_{r0}=0.65 and initial void ratio e_0=0.53. The blue line is the intrinsic WRC. Because of the change in void ratio due to suction loading/unloading, the shapes of the skeleton curves increasingly diverge from the reference intrinsic shape with increasing c_e.

Fig. 10 shows the influences of parameters I_d and I_w on the scanning curve of the WRC. In these element simulations, the initial state is the same, that is, initial suction s_0=15 kPa, the initial degree of saturation S_{r0}=0.55 and the initial void ratio e_0=0.53. The stiffness of the scanning curve of the WRC is higher than that of the skeleton curve at the same suction level, which is the same as the phenomena observed in the experiments by Xiong (2020). In addition, when I_d is smaller than I_w, the stiffness of the drying scanning curve is higher than that of the wetting scanning curve.

4. Performance of the proposed model

A series of water retention, oedometer and triaxial tests on unsaturated Masado (Xiong 2020) were utilized to validate the performance of the proposed models. In these tests, three loading patterns were designed and conducted for the triaxial tests, that is, CS, CDS and u/u conditions.

Certain test results, including water retention and triaxial compression CDS test results, were used to determine the nine material parameters of the constitutive model and the nine WRC parameters by the trial and error fitting method. The values of the parameters are listed in Tables 1 and 2. Moreover, the initial conditions, such as the initial stress, the suction and the degree of saturation, were set to be equal to the values used in the tests, as show in Table 3.

4.1 Water retention tests

In the water retention tests on Masado, the vertical net stress was kept constant, and the suction was loaded and unloaded stepwise between 0 and 250 kPa. Fig. 11 shows a comparison of the test and the simulated WRC of the water retention tests. Generally, the calculated results agree well with the experimental data. It can be observed in Fig. 11(a)

Table 1 Parameters of the WRC of Masado

	Compression	Dilatancy
Saturated degree of saturation S_r^s	0.65	
Residual degree of saturation S_r^r	0.27	
Drying AEV (kPa) S_d	6.00	
Wetting AEV (kPa) S_w	1.00	
Influence of finite deformation on the degree of saturation c_e	0.6	2.0
Shape function parameter c_1	0.011	
Shape function parameter c_2	0.042	
Scanning curve parameter I_d (kPa)	1.6	
Scanning curve parameter I_w (kPa)	1.1	

Table 2 Material parameters of Masado

S Compression index λ	0.089
Swelling index κ	0.008
Critical state parameter R_{cs}	3.65
Void ratio N (p''= 98 kPa on the *N.C.L.*)	0.60
Poisson's ratio ν	0.25
Parameter of overconsolidation a	10.0
Suction parameter b	20.0
Parameter of overconsolidation β	10.0
Parameter of structur m^*	1.00
Void ratio N_r (p''= 98 kPa on the *N.C.L.S.*)	0.63

Table 3 Loading patterns and initial conditions

Case	Loading pattern	Initial stress (kPa)	e_0	s_0 (kPa)	S_{r0}
WR* Case 1	-	σ_v^{net} = 50	0.60	0.0	0.65
WR Case 2		σ_v^{net} = 50	0.61	0.0	0.65
WR Case 3		σ_v^{net} = 50	0.60	0.0	0.65
ODE S_r=0.48	CDS	σ_v^{net} = 20	0.48	50	0.47
ODE S_r=0.44		σ_v^{net} = 20	0.48	50	0.44
ODE S_r=0.38		σ_v^{net} = 20	0.48	50	0.38
TRI s_0=50	CS	σ_3^{net} = 50	0.59	50	0.44
TRI s_0=30		σ_3^{net} = 50	0.60	30	0.51
TRI s_0=10		σ_3^{net} = 50	0.56	10	0.52
TRI s_0=50	CDS	σ_3^{net} = 50	0.59	50	0.52
TRI s_0=30		σ_3^{net} = 50	0.58	30	0.53
TRI s_0=10		σ_3^{net} = 50	0.56	10	0.59
TRI s_0=50	u/u	σ_3^{net} = 50	0.54	50	0.52
TRI s_0=30		σ_3^{net} = 50	0.56	30	0.56
TRI s_0=10		σ_3^{net} = 50	0.55	10	0.61

*WR: water retention test; ODE: oedometer test; TRI: triaxial compression test

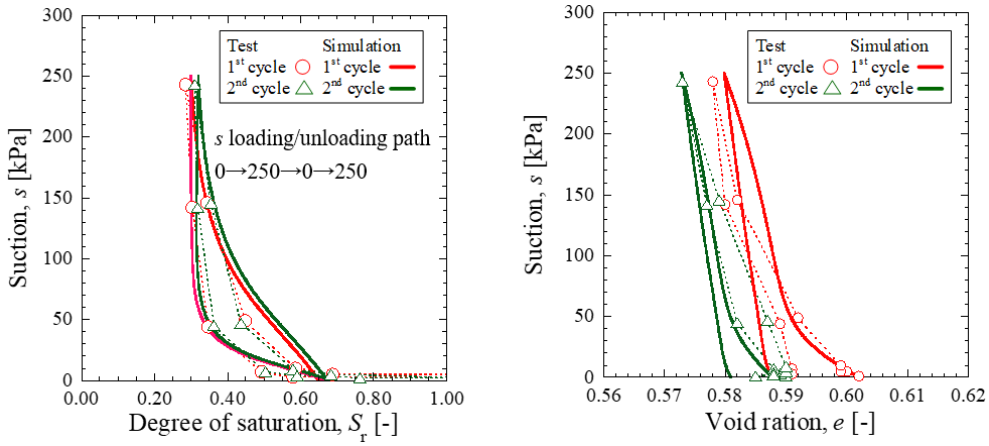

(a) Case 1

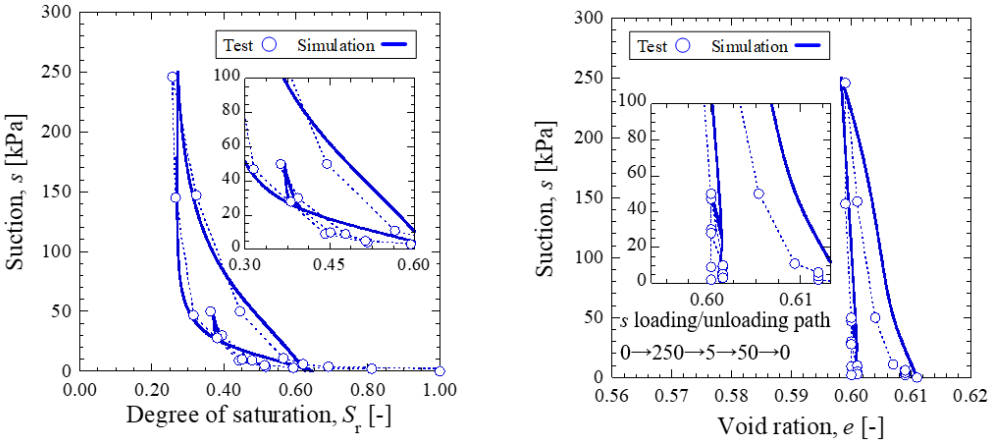

(b) Case 2

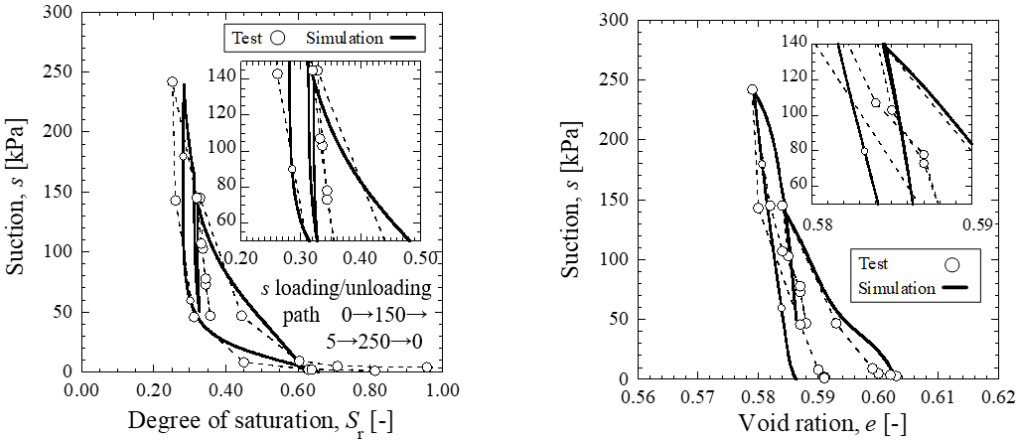

(c) Case 3

Fig. 11 Comparison of the test and simulated WRC in the water retention test

that the proposed model can describe the changes in the skeleton curves with the variations in void ratio. In addition, Fig. 11(b) and 11(c) show that the model can also describe the differences in stiffness between the drying and wetting scanning curves, which is crucial to the proper simulation ofunsaturated soil in triaxial compression tests under different draining and venting conditions.

4.2 Oedometer tests

In the oedometer CDS tests on Masado, the vertical net stress was first loaded to 20 kPa and the suction was loaded to 50 kPa. After the completion of consolidation, the vertical net stress was gradually increased from 20 kPa to 965 kPa at different prescribed degrees of saturation. Fig. 12 shows a comparison of the test and simulated results of unsaturated Masado in the oedometer CDS tests. The changes in suction under the CDS condition were calculated by Eq. (22). As shown in Fig. 12(a), the simulated relationship between the void ratio and vertical skeleton stress agreed quantitatively well with the test results.

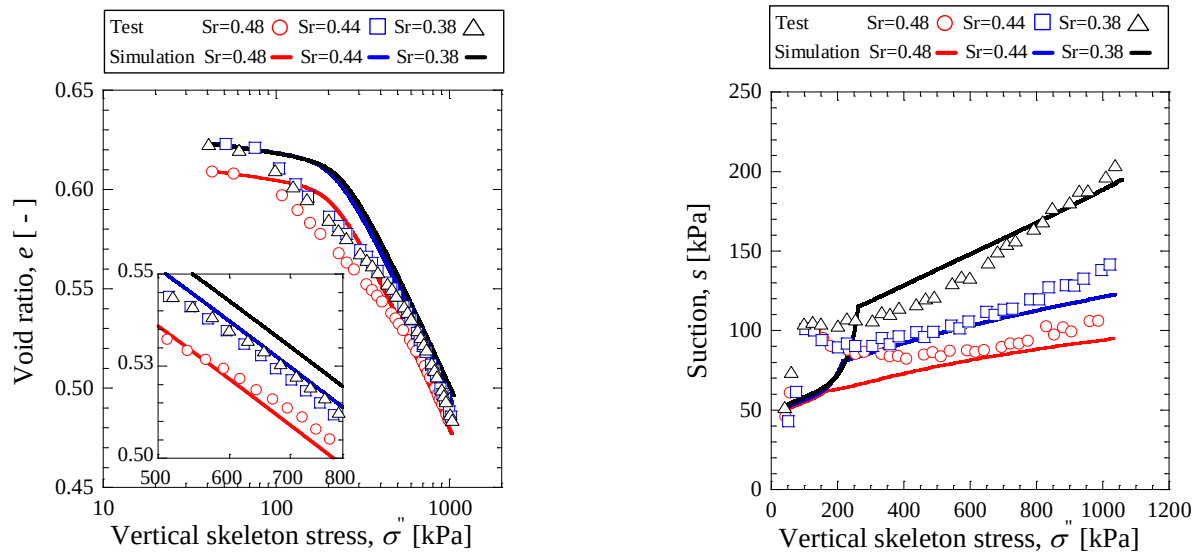

(a) e-σ'' (b) Suction variation

Fig. 12 Comparison of the test and the simulated results of unsaturated Masado in the oedometer CDS tests

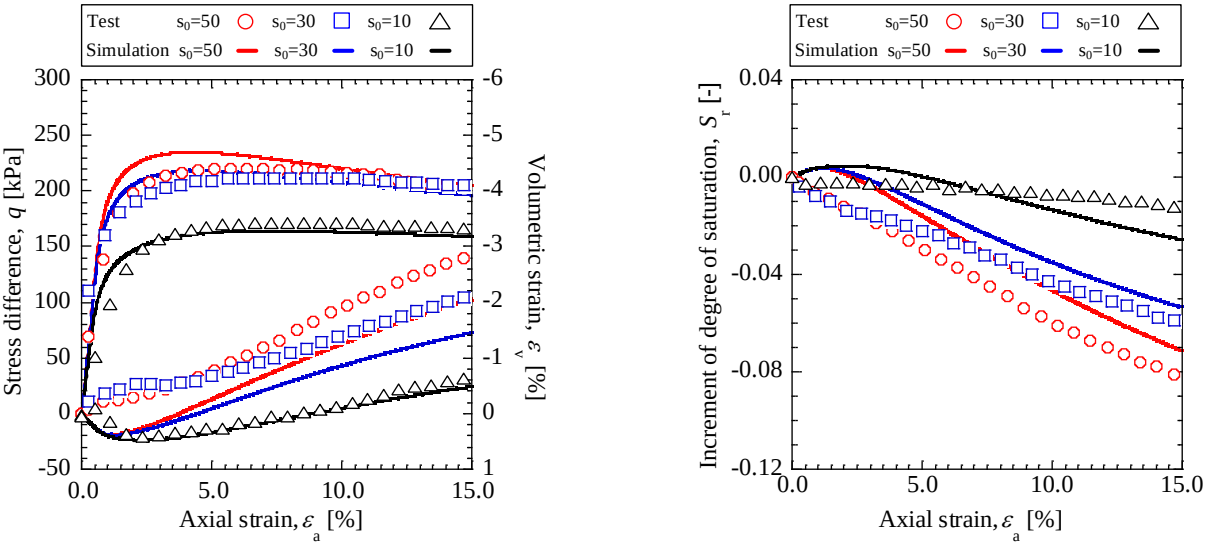

(a) q-ε_v-ε_a (b) S_r variation

Fig. 13 Comparison of the test and simulated results of unsaturated Masado in the triaxial compression CS tests

Although the simulated suction is not coincident with the test result at the beginning of compression, the simulated suction increased with decreasing void ratio and approached the test value at the end of compression, as shown in Fig. 12(b).

4.3 Triaxial compression tests

In the triaxial compression tests on Masado, the specimens were consolidated under the same confining stress but at different suction levels and then sheared under various conditions. Comparisons between the test and simulated results in the triaxial compression tests under CS, CDS and u/u conditions are shown in Figs. 13, 14 and 15, respectively. The changes in saturation under the CDS condition were calculated by Eq. (22), and the variations in suction and degree of saturation under the u/u condition were calculated by Eqs. (23) and (24), respectively. Furthermore, under the u/u condition, the pore air pressure was calculated by the ideal gas law as:

$$u_a V_a = nRT = \text{c} \tag{25}$$

where u_a, V_a, and T are the pore air pressure, volume of gas and absolute temperature, respectively, n is the number of moles of gas, and R is the ideal gas constant. Therefore, the incremental pore water pressure u_w can then be calculated as:

$$du_w = du_a - ds \tag{26}$$

Fig. 13 shows a comparison of the test and the simulated results of unsaturated Masado in the triaxial compression

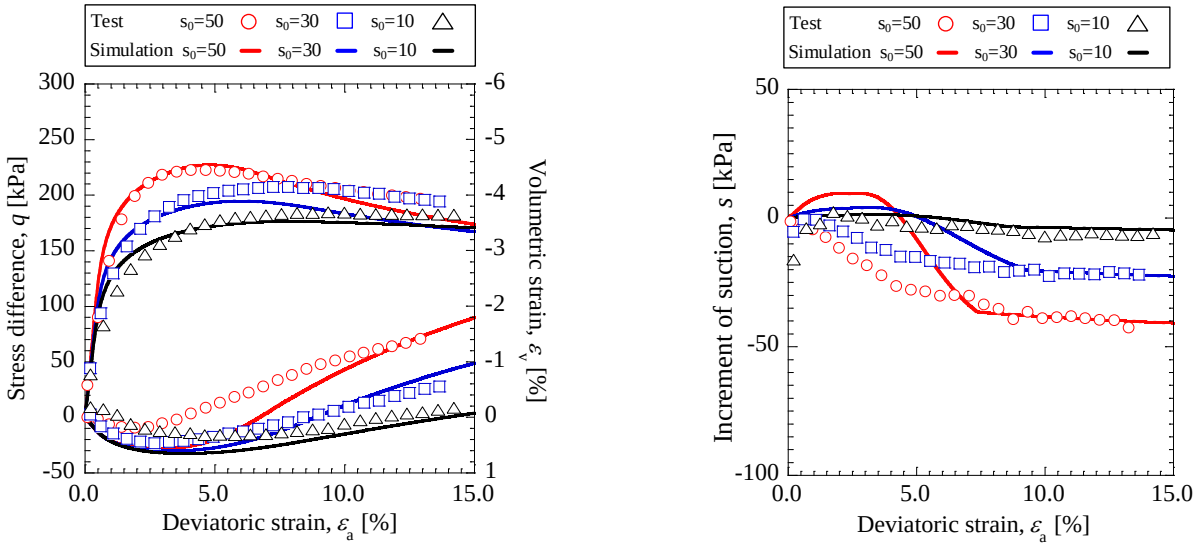

(a) q-ε_v-ε_a (b) Suction variation

Fig. 14 Comparison of the test and simulated results of unsaturated Masado in the triaxial compression CDS tests

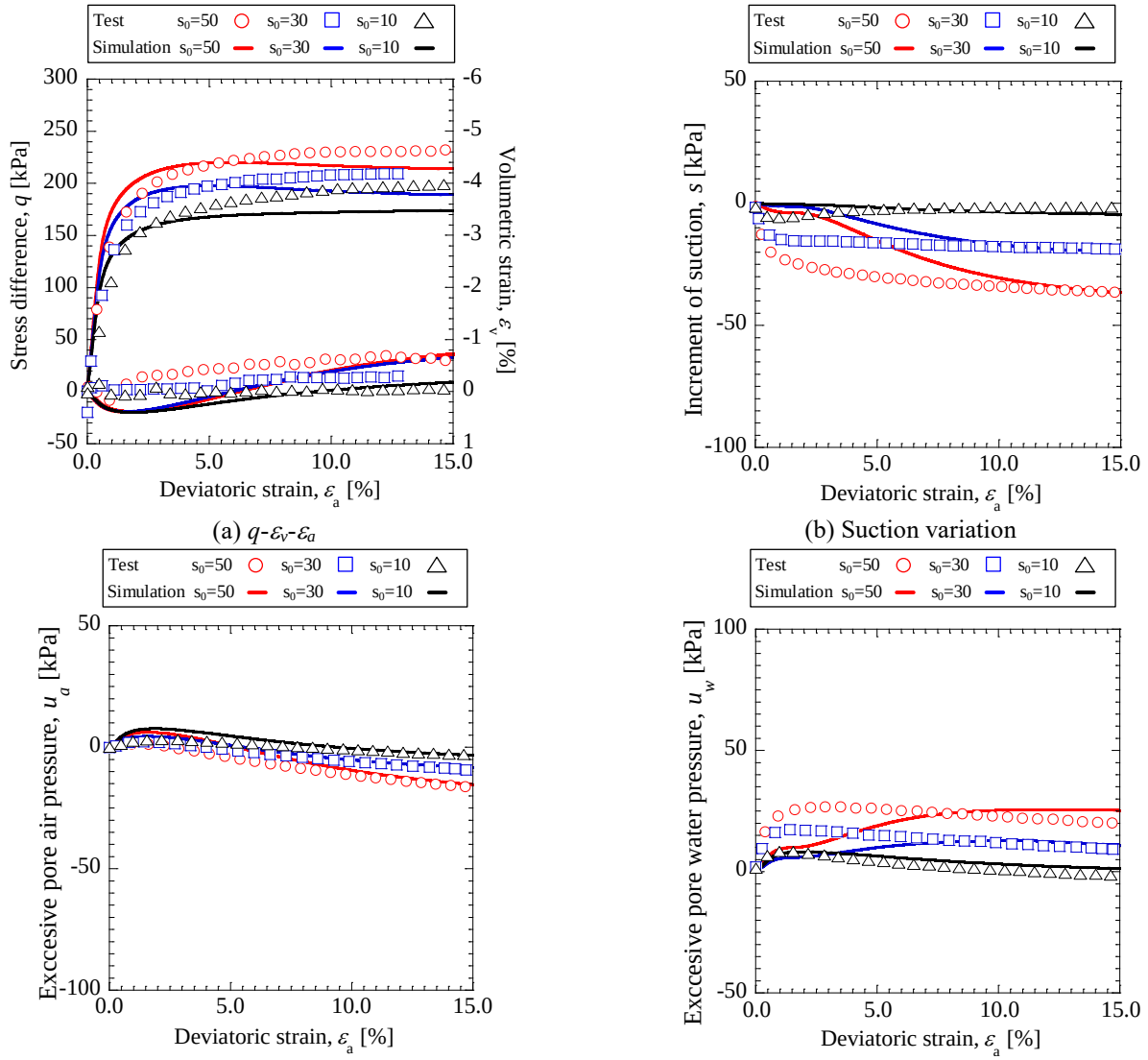

(a) q-ε_v-ε_a (b) Suction variation

(c) Pore air pressure variation (d) Pore water pressure variation (u_{w0}=20 kPa)

Fig. 15 Comparison of the test and simulated results of unsaturated Masado in the triaxial compression u/u tests

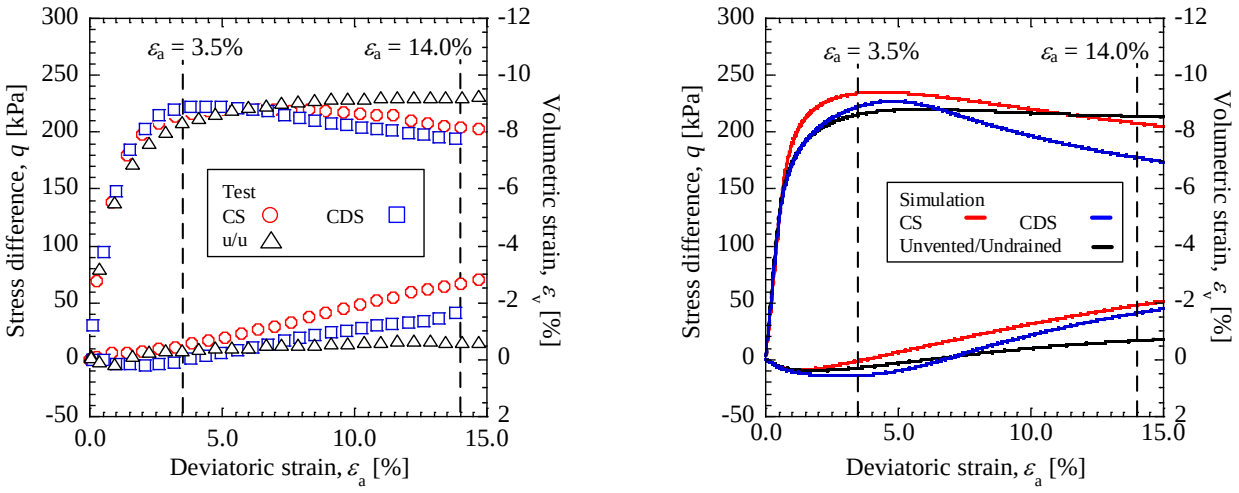

Fig. 16 Comparison of the simulated results in the triaxial compression tests of unsaturated Masado under CS, CDS and u/u conditions (s_0 = 50 kPa)

tests under the CS condition. The simulated stress-strain-dilatancy relation agrees well with the test results, although there exist discrepancies. As shown in Fig. 13(a), the volumetric strain of the test results was dilatant during the whole shearing stage in cases s_0=50 and s_0=30, while the calculated results transitioned from contraction to dilation as the deviatoric strain increased. Furthermore, Fig. 13(b) shows that the proposed model can describe the variations in the degree of saturation under the CS condition. The variations in the degree of saturation have the same tendency as the volumetric strain both in the simulated and test results.

Then, the simulated results under the CDS condition were examined. As shown in Fig. 14(a), the simulated stress-strain-dilatancy relations agree qualitatively well with the test results under the different suction conditions. Moreover, Fig. 14(b) shows that the model is able to capture the overall trend of the tested suction. Since the volume strain transitioned from contraction to dilation, the simulated suction first increased slightly and then decreased. In the case of s_0=50, the decrease rate of the simulated suction slowed down at a deviatoric strain ε_a=7.5%, due to the situation in which point (S_r, s) was transferred from the scanning curve to the main wetting curve. Similar results can also be found in the cases of s_0=30 and 10.

Fig. 15 shows comparisons of the test and simulated results of unsaturated Masado in the triaxial compression u/u tests. A good agreement between the calculated and test results is observed in Fig. 15(a). Compared with the test results, the simulated suction decreased gradually with increasing deviatoric strain in all cases, as shown in Fig. 15(b). Nevertheless, the simulated suction almost reached the same value as the test at the end of shearing with an acceptable accuracy. Moreover, Fig. 15(c) and 15(d) show that the pore air and water pressures can also be described quantitatively using the proposed model.

To confirm the performance of the proposed model under the three different loading conditions, the simulated and test results with the same initial suction (s_0= 50 kPa) are plotted together and compared in Fig. 16. Both the simulated and test results show that the peak strength under the u/u condition at a strain level of ε_a=3.5% is the lowest, while the residual strength under the u/u condition is the highest at a strain level of ε_a=14.0%. In addition, the dilation under CS and u/u conditions is the largest and smallest, respectively, at a strain level of ε_a=14.0%. Similar results can also be found in other tests with different initial suction levels. Although discrepancies still exist, the proposed WRC model coupled with the proposed constitutive model was able to properly describe the influences of the variations in suction and saturation on the strain-stress-dilatancy relationship of unsaturated Masado in triaxial compression tests under different hydraulic/mechanical conditions. It should be emphasised that although the newly proposed WRC model is very simple, it is absolutely impossible to achieve the abovementioned capability without separately considering the influence of suction and void ratio on degree of saturation.

5. Conclusions

In this paper, a saturated/unsaturated constitutive model considering the soil structure and a WRC model considering the volumetric change in soil is newly proposed. The proposed WRC model is incorporated into the constitutive model, and test results from a systematic programme of element tests conducted on unsaturated Masado (Xiong, 2020) are used to validate the proposed model. The following conclusions can be drawn in this study.

Based on the experimental evidence, it is assumed in this paper that if only subjected to volumetric deformation, the shape of the intrinsic WRC at any void ratio does not change, but the curve only shifts parallel to the S_r axis in S_r-s space.

Based on the aforementioned assumption, the original WRC model proposed by Zhang and Ikariya (2011) is modified by adding simplified linear functions of the increments in the degree of saturation, suction and void ratio. Using these newly proposed formulations, three

characteristic scanning curves under specific conditions are also proposed for the WRC model.

By comparing the test and calculated results, it is found that on the whole, the calculated results agree well with the test results along all loading patterns. The proposed model has a satisfactory accuracy for describing the hydraulic/mechanical behaviour of unsaturated Masado under CS, CDS and u/u conditions. Of course, all the simulations are conducted under the condition that the material parameters are the same for all loading patterns. In addition, without this newly proposed WRC model, it is absolutely impossible to achieve the abovementioned capability.

There are still discrepancies between the test and calculated suction-saturation relations, which is thought to be caused by the incomplete fitting between the test and calculated volumetric strains. To improve the accuracy of the proposed model, further refinements should be attained in both testing and modelling.

Acknowledgments

This research was substantially supported by the Natural Science Foundation of China (41731283), the Natural Science Foundation of Ningbo (2018A610430) and the Natural Science Foundation of Zhejiang Province (LY19E080012). Financial support from the Grant-in-Aid Scientific Research (B), No.17H03304, JSPS, is also greatly appreciated.

References

Asaoka, A., Nakano, M. and Noda. T. (1998), "Super loading yield surface concept for the saturated structured soils", *Proceedings of the 4th European Conference on Numerical Methods in Geotechnical Engineering NUMGE98*, Udine, Italy, October.

Asaoka, A., Nakano, M. and Noda, T. (2000), "Superloading yield surface concept for highly structured soil behavior", *Soils Found*., **40**(2), 99-110. https://doi.org/10.3208/sandf.40.2_99.

Burton, G.J., Pineda, J.A., Sheng, D., Airey, D.W. and Zhang, F. (2016), "Exploring one-dimensional compression of compacted clay under constant degree of saturation paths", *Géotechnique*, **66**(5), 435-440. https://doi.org/10.1680/jgeot.14.P.181.

Gallipoli, D. (2012), "A hysteretic soil-water retention model accounting for cyclic variations of suction and void ratio", *Geotechnique*, **62**(7), 605-616. https://doi.org/10.1680/geot.11.P.007.

Gallipoli, D., Bruno, A.W., D'onza, F. and Mancuso, C. (2015), "A bounding surface hysteretic water retention model for deformable soils", *Géotechnique*, **65**(10), 793-804. https://doi.org/10.1680/jgeot.14.P.118.

Gallipoli, D., Wheeler, S.J. and Karstunen, M. (2003), "Modelling the variation of degree of saturation in a deformable unsaturated soil", *Géotechnique*, **53**(1), 105-112. https://doi.org/10.1680/geot.2003.53.1.105.

Gao, Y., Sun, D., Zhou, A. and Li, J. (2018), "Effect of stress state on soil-water retention and its application on the strength prediction", *Geotechnique Lett*., **8**(4), 324-329. https://doi.org/10.1680/jgele.18.00159.

Gao, Y., Li, Z., Sun, D.A. and Yu, H.H. (2021), "A simple method for predicting the hydraulic properties of unsaturated soils with different void ratios", *Soil Till. Res*., https://doi.org/10.1016/j.still.2020.104913.

Chen, B., Ding, X., Gao, Y., Sun, D.A. and Yu, H. (2020), "Hydro-mechanical behavior of compacted silt over a wide suction range", *Geomech. Eng*., **22**(3), 237-244. https://doi.org/10.12989/gae.2020.22.3.237.

Hashiguchi, K., and Ueno, M. (1977), "Elastoplastic constitutive laws of granular material, constitutive equations of soils", *Proceedings of the 9th International Conference on Soil Mechanics and Foundation Engineering*, Tokyo, Japan, July.

Henkel, D.J. (1960), "The shear strength of saturated remoulded clays", *Proceedings of the Conference on Shear Strength of Cohesive Soils*, Boulder, Colorado, U.S.A., June.

Hu, R., Chen, Y.F., Liu, H.H. and Zhou, C.B. (2013), "A water retention curve and unsaturated hydraulic conductivity model for deformable soils: Consideration of the change in pore-size distribution", *Géotechnique*, **63**(16), 1389-1405. https://doi.org/10.1680/geot.12.P.182.

Kawamura, S. and Miura, S. (2018), "Mechanical behavior of decomposed granite soils in Hokkaido and its evaluation", *Jap. Geotech. J*., **13**(2), 159-170, https://doi.org/10.3208/jgs.13.159 (In Japanese).

Khoshghalb, A., Pasha, A.Y. and Khalili, N. (2015), "A fractal model for volume change dependency of the water retention curve", *Géotechnique*, **65**(2), 141-146. https://doi.org/10.1680/geot.14.T.016.

Li, J. and Cameron, D.A. (2002), "Case study of courtyard house damaged by expansive soils", *J. Perform. Constr. Fac*., **16**(4), 169-175. https://doi.org/10.1061/(ASCE)0887-3828(2002)16:4(169).

Maqsoud, A., Bussière, B., Aubertin, M. and Mbonimpa, M. (2012), "Predicting hysteresis of the water retention curve from basic properties of granular soils", *Geotech. Geol. Eng*., **30**(5), 1147-1159. https://doi.org/10.1007/s10706-012-9529-y.

Miller, G.A., Khoury, C.N., Muraleetharan, K.K., Liu, C. and Kibbey, T.C. (2008), "Effects of soil skeleton deformations on hysteretic soil water characteristic curves: Experiments and simulations", *Water Resour. Res*., **44**(5), 1-10. https://doi.org/10.1029/2007WR006492.

Murata, H., Hyodo, M. and Yasufuku, N. (1988), "Prediction of stress-strain behaviour of undisturbed "Masado"", *Technol. Rep. Yamaguchi Univ*., **4**(2), 161-170.

Nuth, M. and Laloui, L. (2008), "Advances in modelling hysteretic water retention curve in deformable soils", *Comput. Geotech*., **35**(6), 835-844. https://doi.org/10.1016/j.compgeo.2008.08.001.

Pasha, A.Y., Khoshghalb, A. and Khalili, N. (2017), "Hysteretic model for the evolution of water retention curve with void ratio", *J. Eng. Mech*., **143**(7), 04017030. https://doi.org/10.1061/(ASCE)EM.1943-7889.0001238.

Romero, E., Della Vecchia, G. and Jommi, C. (2011), "An insight into the water retention properties of compacted clayey soils", *Géotechnique*, **61**(4), 313-328. https://doi.org/10.1680/geot.2011.61.4.313.

Salager, S., Nuth, M., Ferrari, A. and Laloui, L. (2013), "Investigation into water retention behaviour of deformable soils", *Can. Geotech. J.*, **50**(2), 200-208. https://doi.org/10.1139/cgj-2011-0409.

Sehara, Y., Suzuki, M., Yamamoto, T., Terayama, T., Tomokiyo, T. and Kochi, Y. (2006), "Slope disasters caused by typhoon No. 14 of 2005 in Yamaguchi Prefecture", *Soils Found.*, **46**(6), 817-830, https://doi.org/10.3208/sandf.46.817.

Seiphoori, A., Ferrari, A. and Laloui, L. (2014), "Water retention behaviour and microstructural evolution of MX-80 bentonite during wetting and drying cycles", *Géotechnique*, **64**(9), 721-734. https://doi.org/10.1680/geot.14.P.017.

Sheng, D. (2011), "Review of fundamental principles in modelling unsaturated soil behaviour", *Comput. Geotech*., **38**(6), 757-776. https://doi.org/10.1016/j.compgeo.2011.05.002.

Sheng, D., Sloan, S. and Gens, A. (2004), "A constitutive model

for unsaturated soils: Thermomechanical and computational aspects", *Comput. Mech.*, **33**(6), 453-465. https://doi.org/10.1007/s00466-003-0545-x.

Sheng, D., and Zhou, A.N. (2011), "Coupling hydraulic with mechanical models for unsaturated soils", *Can. Geotech. J.*, **48**(5), 826-840. https://doi.org/10.1139/t10-109.

Sugii, T., Yamada, K. and Kondou, T. (2002), "Relationship between soil-water characteristic curve and void ratio", *Proceeding of the 3rd International Conference on Unsaturated Soils*, Recife, Brazil, March.

Sun, D.A., Sheng, D.C., Cui, H.B. and Sloan, S.W. (2007), "A density-dependent elastoplastic hydro-mechanical model for unsaturated compacted soils", *Int. J. Numer. Anal. Met.*, **31**(11), 1257-1279. https://doi.org/10.1002/nag.579.

Sun, G., Zheng, H., Tang, H. and Dai, F. (2016), "Huangtupo landslide stability under water level fluctuations of the Three Gorges reservoir", *Landslides*, **13**(5), 1167-1179. https://doi.org/10.1007/s10346-015-0637-7.

Sun, W., Sun, D.A., Fang, L. and Liu, S. (2014), "Soil-water characteristics of Gaomiaozi bentonite by vapour equilibrium technique", *J. Rock Mech. Geotech. Eng.*, **6**(1), 48-54. https://doi.org/10.1016/j.jrmge.2013.12.004.

Tan, F., Zhou, W.H. and Yuen, K.V. (2016), "Modeling the soil water retention properties of same-textured soils with different initial void ratios", *J. Hydrol.*, **542**, 731-743. https://doi.org/10.1016/j.jhydrol.2016.09.045.

Tarantino, A. (2009), "A water retention model for deformable soils", *Géotechnique*, **59**(9) 751-762. https://doi.org/10.1680/geot.7.00118.

Tsuchida, T., Athapaththu, A.M.R.G., Kano, S. and Suga, K. (2011), "Estimation of in-situ shear strength parameters of weathered granitic (Masado) slopes using lightweight dynamic cone penetrometer", *Soils Found.*, **51**(3), 497-512. https://doi.org/10.3208/sandf.51.497.

van Genuchten, M.T. (1980), "A closed-form equation for predicting the hydraulic conductivity of unsaturated soils", *Soil Sci. Soc. Am. J.*, **44**(5), 892-898. https://doi.org/10.2136/sssaj1980.03615995004400050002x.

Vaunat, J., Romero, E. and Jommi, C. (2000), "An elastoplastic hydromechanical model for unsaturated soils", *Proceedings of the International Workshop on Unsaturated Soils*, Trento, Italy, April.

Wijaya, M., and Leong, E.C. (2017), "Modelling the effect of density on the unimodal soil-water characteristic curve", *Géotechnique*, **67**(7), 637-645. https://doi.org/10.1680/jgeot.15.P.270.

Xiong, Y.L., Ye, G.L., Xie, Y., Ye, B., Zhang S. and Zhang F. (2019), "A unified constitutive model for unsaturated soil under monotonic and cyclic loading", *Acta Geotechnica*, **14**(2), 313-328. https://doi.org/10.1007/s11440-018-0754-2

Xiong, X. (2020), "Modeling of hydro-mechanical behavior of unsaturated soils considering finite deformation and its application to unsaturated landslide dam stability", Ph.D. Dissertation, Nagoya Institute of Technology, Nagoya, Japan.

Zhang, F. and Ikariya, T. (2011), "A new model for unsaturated soil using skeleton stress and degree of saturation as state variables", *Soils Found.*, **51**(1), 67-81. https://doi.org/10.3208/sandf.51.67.

Zhou, A. and Sheng, D. (2015), "An advanced hydro-mechanical constitutive model for unsaturated soils with different initial densities", *Comput. Geotech.*, **63**, 46-66. https://doi.org/10.1016/j.compgeo.2014.07.017.